OPEN ACCESS

Kashf Journal of Multidisciplinary Research
Vol:01 Issue:10 2024
P-ISSN: 3007-1992 E-ISSN: 3007-200X
https://kjmr.com.pk

INTELLIGENT MELANOMA DETECTION BASED ON PIGMENT NETWORK

Inzamam Shahzad
Department School Of Computer Science And School Of Cyberspace Science, Xiangtan University, Xiangtan Hunan, China

Salahuddin
Department of Computer Science, NFC Institute of Engineering and technology, Multan, Pakistan.

Abdul Manan Razzaq
Department of Computer Science, NFC Institute of Engineering and technology, Multan, Pakistan.

Mubashar Hussain
Department of computer science, university of Engineering and technology Lahore Pakistan.

Meiraj Aslam
Department of Computer Science, NFC Institute of Engineering and technology, Multan, Pakistan.

Prince Hamza Shafique
Department of Computer Science, NFC Institute of Engineering and technology, Multan, Pakistan.

Syed Shahid Abbas
Department of Computer Science, NFC Institute of Engineering and technology, Multan, Pakistan.

Article Info

Received: 16th Oct, 2024
Review 1: 19th Oct, 2024
Review 2: 23th Oct, 2024
Published: 26th Oct, 2024

Abstract

Early detection of melanoma, the deadliest form of skin cancer, is critical for effective treatment. Detecting skin lesions accurately from dermoscopic images remains challenging, with the pigment network being a crucial indicator for melanoma detection. The accurate identification of pigment networks in dermoscopic images is difficult due to image noise and unwanted hair artifacts, which can obscure meaningful diagnostic features. To address these challenges, this thesis proposes novel image processing approaches for computer-aided pigment network detection. These methods aim to enhance image clarity by filtering out unwanted elements and converting images into binary formats, facilitating more precise analysis. Initially, preprocessing involves filtering dermoscopic images to remove noise and unwanted hair artifacts, enhancing image quality for more effective analysis. Subsequently, binary conversion and creation of binary masks further refine image clarity. The final step involves detecting pigment networks and calculating key features such as diameter and radius to assess melanoma presence. The proposed method achieves comparable accuracy and efficiency to existing algorithms. It demonstrates an average precision of 0.89 and average recall of 0.87, with an overall accuracy of 85.5%.

Keywords: *Deep Learning, Melanoma Detection, Pigment Network, Diffusion.*

1. Introduction

Skin cancer is the most common form of human cancer if melanoma, basal and squamous cell skin cancers are considered. Cancer is the second leading cause of deaths in the entire world. The annual ratios of all types of skin cancer are growing every year. World Health Organization estimates 8.8 million died due to cancer in 2015 in all over the world. Malignant melanoma, the deadliest form of skin cancer, is one of the most rapidly increasing cancers in the world [1]. 101,000 peoples are dying from cancer in Pakistan per year [3]. Two main reasons of this disease are the depletion of ozone layer caused by pollution and second is the extreme exposure to sun.

Metastatic melanoma is very hard to treat, so the best treatment is still early diagnosis and prompt surgical excision of the primary cancer so that it can be fully excised while it is still localized [2]. Therefore, advances in computer-aided diagnostic methods can aid self-examining approaches based on digital images, and may significantly reduce the mortality. This thesis investigates and reviews important features of automated analysis of skin lesions using digital dermoscopic images and proposes a novel approach for automated recognition of the melanoma.

Dermoscopy is a non-invasive investigative technique which is used to see a variation of patterns and structures in skin lesions that are not visible to the naked eye. It has different names like epiluminescence microscopy (ELM), dermoscopic or skin surface microscopy. The dermoscopic procedure consists of placing oil, alcohol or even water on the surface of the lesion. These solutions make epidermis more transparent to light and eradicate part of the surface reflection. After placing the liquid, the lesion is examined using a dermoscopic, a stereomicroscope, a camera or a digital imaging system.

The objective of research is to find better and more efficient way to automatically detect early melanoma. Method focuses on preprocessing stage, analysis of color variegation, border irregularity and symmetry of malignant tumor. Addition to it, Proposed method aims is to ease the doctor role in the detection of melanoma by providing better results so that patient can be diagnosed and cure at early stage.

2. Method, and materials

Automatic detection of melanoma has received certain recent attention. A lot of work has done to detect melanoma at early stage. We proposed a new approach for classification and segmentation of skin lesion. First of all, dermoscopic images are filtered to remove unwanted hair and noise. Then segmentation is applying to extract lesion area from image. Segmentation performance is also compared with other measures, result was appreciable. The extracted lesion part is represented by color and texture features. SVM and k-NN are used with their fusion for the purpose of classification using extracted features. Figure 1 presents the flowchart diagrams of proposed methodology.

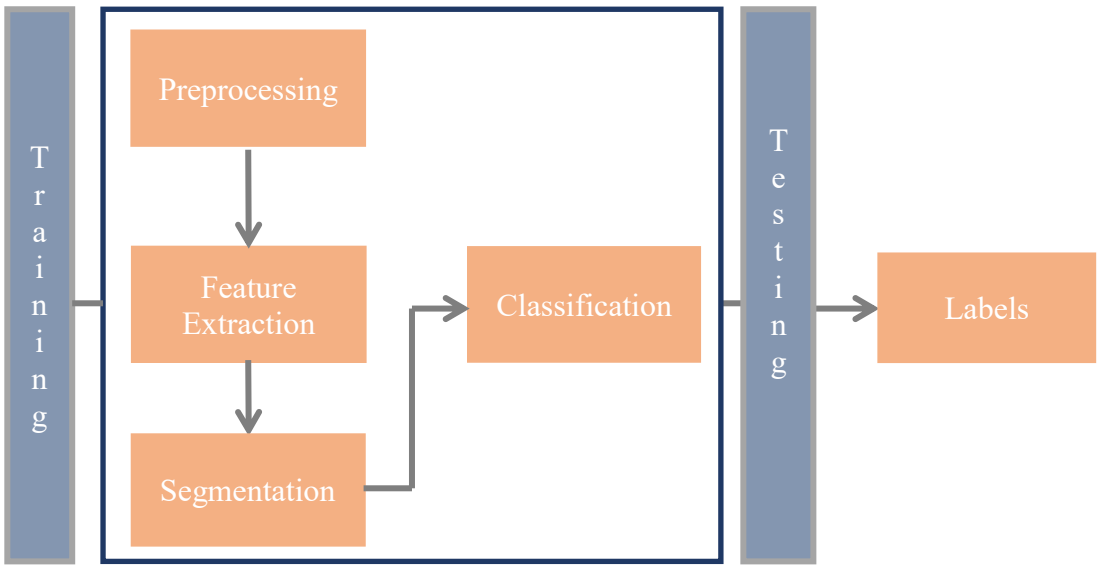

2.1. Preprocessing

The first step in the automated analysis of skin lesion images is the preprocessing of an image. The preprocessing techniques will be different for different application based on the desired dataset of an image. The key goal of preprocessing techniques is image enhancement and image restoration.

2.1.1. Gaussian Smoothing

To remove noise of image, filtering technique known as Gaussian smoothing is applied. Gaussian filter is a non-uniform low pass filter. To perform this task, 3×3 Gaussian filter is used to smoothen the image. The degree of smoothing image is determined by the standard deviation of the Gaussian. Gaussian smoothing blurs the image and removes noise and hairs. Gaussian function is given below eq (1). Where σ standard deviation of distribution and x, y is axis.

$$G(x,y)=\frac{1}{2\pi\sigma^2}e^{-\frac{x^2+y^2}{2\sigma^2}} \quad (1)$$

(a) Original Image

(b) Image after gaussion filter

Figure 2 Process Image

2.2. Morphological Operations

After Gaussian filtering is applied, for enhancement of filtered image, morphological operations like erosion and dilation are applied. Erosion and dilation are applied to the filtered image after Gaussian smoothing.

2.2.1. Erosion

Erosion is a morphological operation applied on image. In morphological operations, a structuring element is applied to an input image, and it creates an equal size of output image. In a morphological operation, the value of every pixel in the output image is grounded on an association of the corresponding pixel in the input image with its neighbors. In morphological erosion removes pixels on object borders. The number of pixels removed from image depends upon the size of structure element. Erosion of image *I* by a structure element *S* is denoted as eq (2).

$$I \ominus S \quad (2)$$

2.2.2. Dilation

After erosion, second morphological operation dilation is applied to image. Dilation is inverse of erosion. Dilation adds the pixel on the border of image. The value of the output pixel is the maximum value of all the pixels in the input pixel's neighborhood. In a binary image, if any of the pixels is set to the value 1, the output pixel is set to 1. Dilation of image I by structuring element S is shown below eq (3).

$$I \oplus S \quad (3)$$

2.3. Segmentation

There are many methods used for segmentation of images. The segmentation of skin lesions is a fundamental initial step in the method of automatically diagnosing melanoma. Incorrect segmentations will disturb all remaining processes like feature extraction, feature selection and the lesion detection. Region based segmentation is used for segmentation process.

2.3.1. Region Growing and Splitting

This algorithm begins with a set of "seed" points and from these; regions will grow by adding to every seed point those neighboring pixels that have same properties. At the begin image is considered as one region. It will look for groups of pixels of similar attributes and divided the image into a set of minor regions. Then a uniformity test is applied to every region: if the test fails, the region is divided into small elements. The uniformity test is applied once more; this is repeated till al1 regions are uniform, therefore splitting the image into smaller regions.

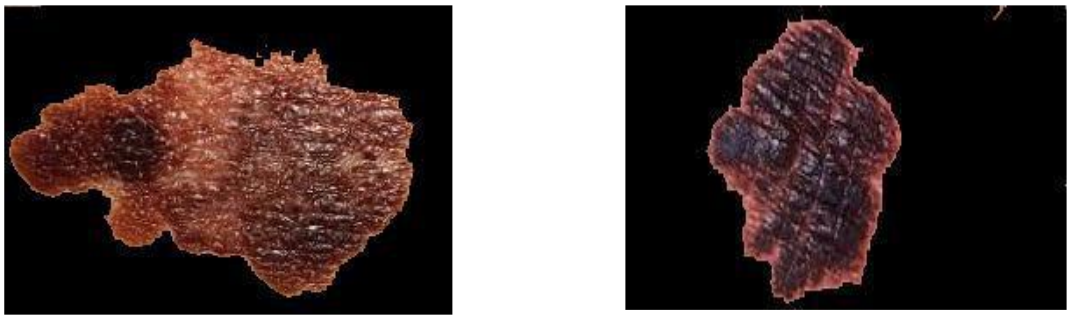

Figure 3 Example of segmented images

2.4. Feature Extractions

Features have a very significant role in the field of image processing. Feature extraction techniques are applied to acquire features which are useful for classification and recognition of images. Feature extraction techniques are useful in several image processing applications like face recognition, iris recognition, skin cancer detection etc. Behavior of an image, efficiency in classification is properties defied and observed by feature extraction. Main purpose of feature extraction is to obtain most relevant information like shape, color of an image so that it can be classified. When an input data for an algorithm is large enough for processing, then this data is transformed into reduced set of features (also called feature vector) [24]. This transferring of input into set of features is also known

as feature extraction. In proposed method color and texture features are used to present skin lesion area. Because the fact is that color and texture are only properties that dominating in the lesion area.

2.4.1. Color Feature

In order to measure the color existing in skin lesion, four statistics like mean, standard deviation, variance and skewness are extracted from skin lesion over individual channels of six different color spaces: RGB, HSV, YCbCr, NTSc, CIE L*u*v and CIE L*a*b. These four features are also called color moments.

Let Pi be the ith pixel of a color channel P of an image k with M pixel in color space then the four-color moments are defined as Moment 1-Mean is the average color value in channel as eq (4)

$$\mu = \frac{1}{M}\sum_{i=1}^{M} p \qquad (4)$$

Moment 2- Standard deviation is the square root of variance of distribution that is written below eq (5)

$$\sigma = \sqrt{\frac{1}{M}\sum_{i=1}^{M}(Pi - \mu)^2} \qquad (5)$$

Moment 3-Skewness is the measure of degree of asymmetry in the distribution as eq (6)

$$S = \sqrt[3]{\frac{1}{M}\left(\sum_{i=1}^{M}(p_i - \mu)^3\right)} \qquad (6)$$

Moment 4- Variance is variation of color distribution, which is given below eq (7)

$$V = \frac{1}{M}\sum_{i=1}^{M}(p_i - \mu)^2 \qquad (7)$$

The above-mentioned moments described four features which are computed over all the channels and give results in 72 color features obtained by following pattern (6 color spaces) × (3 channels for each color space) × (4 features).

2.4.2. Texture Feature

Texture is one of important feature used to recognize objects in an image. Image texture provides us facts about the spatial arrangement of color or intensities in an image or particular area of an image. To obtain texture features in the skin lesion, a set of statistical feature descriptor based on gray level occurrence matrix are used also abbreviated as GLCM. The GLCM functions describe the texture of an image by calculating how frequently pairs of pixels with specific values and in a specified spatial relationship take place in an image. Gray level occurrence matrix-based reports are well-known and commonly used for texture analysis of skin lesion. Co-occurrence texture features are

extracted from an image in two phases. In first phase pairwise spatial concurrence of pixels is isolated by a precise angle and their distance are calculated by using gray level occurrence matrix. In second step, GLCM is used to measure a set of scalar quantities which differentiate several features of original texture. GLCM is m × m square matrix, where m belongs to number of different gray levels in an image. The *graycomatrix* function generates a gray level co-occurrence matrix (GLCM) by computing exactly how often a pixel with the intensity value *i* occurs in a precise spatial relationship to a pixel with the value *j*. By default, the spatial relationship is well-defined as the pixel of interest and the pixel to its adjacent right (horizontally adjacent), but other spatial relationships between the two pixels can also be specified. Each element (*i*,*j*) in the resultant GLCM is basically the sum of the number of times that the pixel with value *i* occurred in the identified spatial relationship to a pixel with value *j* in the input image.

2.5. kNN and SVM classifier

In classification, kNN is a technique for classifying grounded on closest training samples in the feature space. It is the well-known and modest of all algorithms for predicting the class of a test example. kNN provide class labels at the end results. It predicts the class label, according to nearest neighbor of point of interest. This algorithm holds next three steps to classify.

- First of all, calculate distance of all training vector to test vector
- Then its picks the k closet vector
- Calculate average

If value of k is chosen 1, object is assigned the label of its nearest neighbor. The best value for k depends upon data. Generally, if larger value of k decreases the noise effect but also make boundaries among classes less different. In order to calculate the distance of training vector to test vector distance measure such as Euclidean distance, City block distance, and correlation can be used. Most common distance measure is Euclidean distance. The accuracy of kNN algorithm can be degraded in the presence of noise or irrelevant features. Training phase of kNN consist of storing the feature vector and class label of training data.

SVM stands for Support Vector Machine, it was proposed by Cortes and Vapnik in 1993. It is a powerful supervised learning tool for classification. SVM is supervised learning algorithm which is characterized by considerable resistance to over fitting, a long standing and inherent problem algorithm. This excessive feature of SVM is the fact that it pays structural risk minimization problem rather than empirical risk minimization process, which reduces the upper bound on generalization error. Generally, the SVM is considered for dichotomic classification (binary classification problem with two classes). So, the final aim of SVM is to find the optimal dichotomic hyper plane that can maximize the margin of two classes. To achieve this purpose, on both side of this hyper plane, two parallel hyper planes are created. Then, SVM attempts to discover the splitting hyper plane that make the most of the distance between the two parallel hyper planes. Instinctively an optimized hyper plane separation having largest distance is achieved. In the proposed approach, two classes of lesion are created. The SVM classifier with radial basis function (also called RBF) kernel and default parameters is trained using local features extracted from skin lesion images.

Use of RBF kernel rather than other kernel has benefited that it limit training data to lie in specific boundary. It's another advantage is that it has lesser computational and numerical difficulties. Finally, in test phase, unseen skin lesion sample is given to train SVM for the purpose of classification based on extracted local features. For multiclass SVM we have considered chi-square kernel in the form of Equation 3-8, here X, Y are N dimensional inputs and K is the kernel function that maps the data from N dimensional space to M dimension space, usually M is much larger than N. Studies show that if features are in the form of a histogram, the Chi-square kernel yields better performance as compared to the others kernels [29].

$$K(X,Y) = \sum_i x_i \frac{y_i}{x_i + y_i} \tag{8}$$

3. Implementation and result

In this section, experimental results are presented in order to demonstrate the performance of proposed system. To assess the performance of proposed approach, different experiments have been carried out at large data set. The proposed algorithm is implemented in MATLAB 8.1.0 (R2013a) and the performance of proposed algorithm is evaluated through various validity measures.

3.1. Dataset Detail

This research utilized data set [7, 27, 28] publicly available to test the proposed methodology. To evaluate the performance of proposed approach, different experiments have been carried out at large data set of digital images acquired from different sources. Figure 4 presents the samples imaged of dataset.

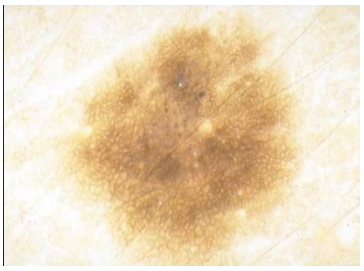

(a)

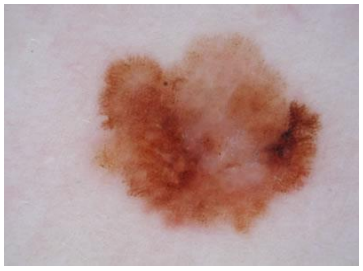

(b)

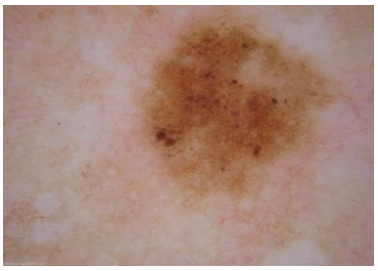

(c)

(d) (e) (f)

Figure 4 Example of original images

3.2. Performance analysis on dermoscopic image

The experimental work is carried out on various dermoscopy images to analyze the performance of proposed algorithm and results are compared with other algorithms. Figure 5 presents the a is gray scale image of original image (a), b is gray scale mage of original image (b), c is the gray scale image of original image (c), d is the gray scale image of original image (d), e is gray scale image of original image (e), f is gray scale image of original image.

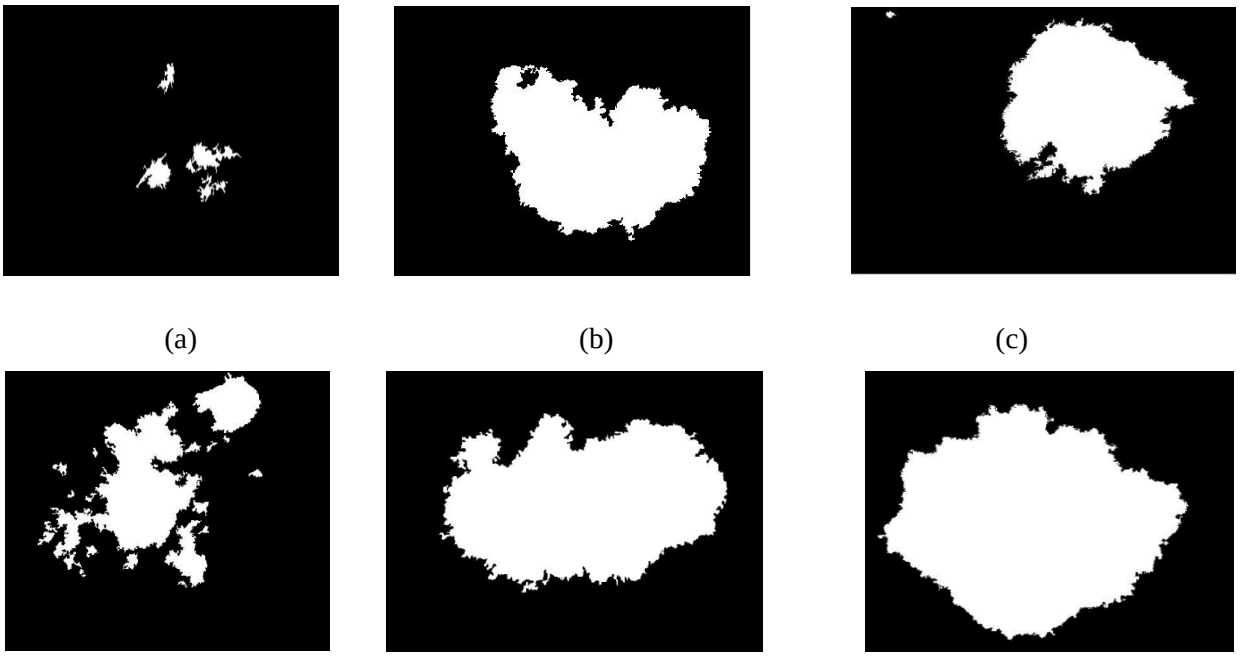

(a) (b) (c)

(d) (e) (f)

Figure 5 Example of gray Scale images

Figure 6 presents the binary image of original image (a), b is the binary image of original image (b), c is the binary image of original image (c), d is the binary image of original image (d), e is the binary image of 4-1(e), f is the binary image of original image (f).

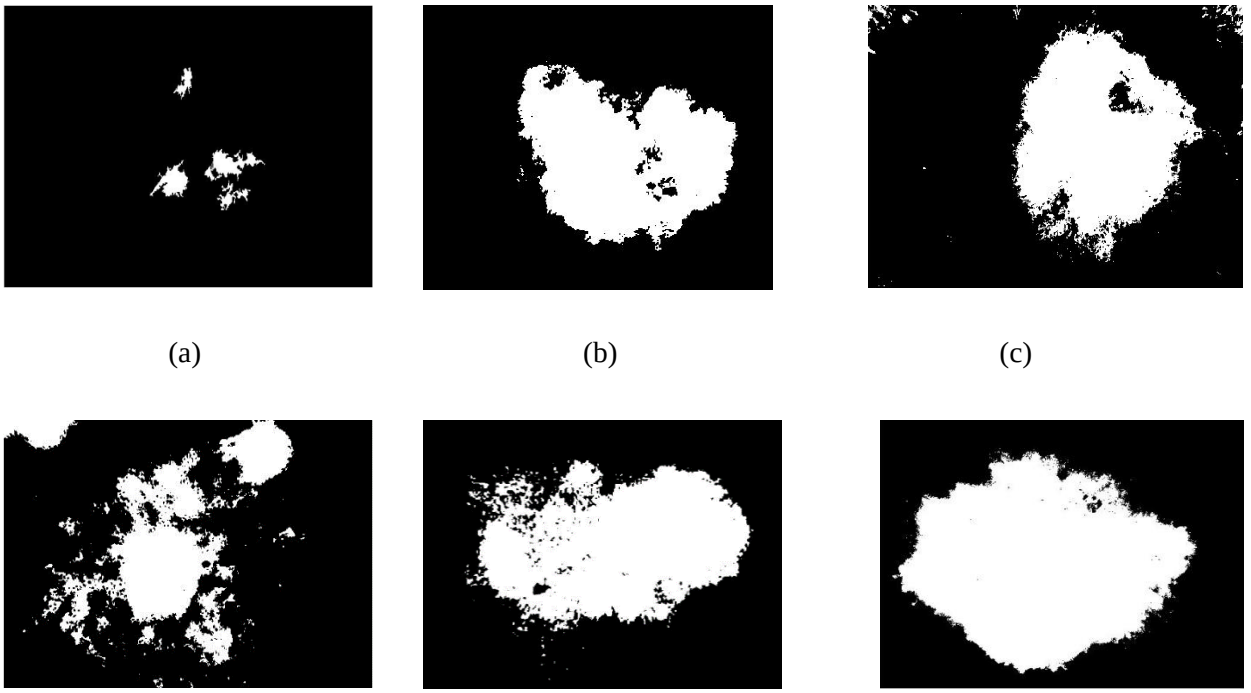

(a) (b) (c)

(d) (e) (f)

Figure 6 Example of binary Scale images

After converting melanoma image to binary image, binary mask for images is generated as shown below Figure 7. Figure presents the binary mask of image original image (a), b is the binary mask of image original image (b), c is the binary mask of image original image (c), d is the binary mask of image original image (d), e is the binary mask of image 4-3(e), f is the binary mask of image original image (f).

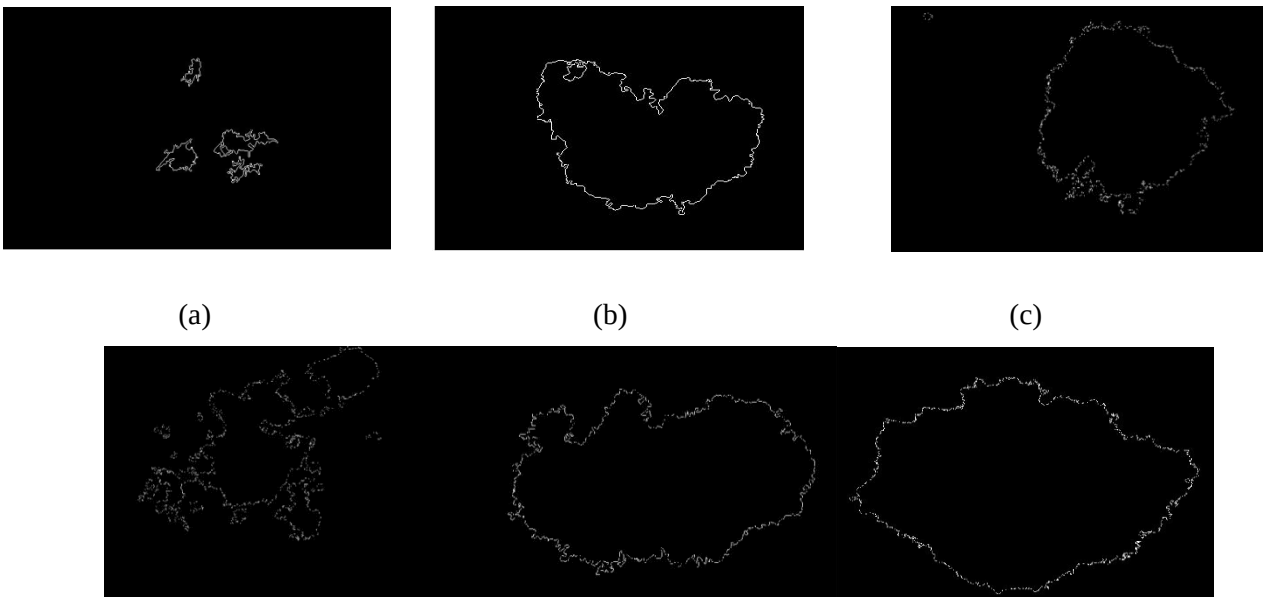

(a) (b) (c)

(d) (e) (f)

Figure 7 Example of binary Mask images

Figure presents metric calculated for image 4-4(a), b is metric calculated for image original image (b), c is metric calculated for image original image (c), d is metric calculated for image original image (d), e is metric calculated for image 4-4(e), f is metric calculated for image original image (f).

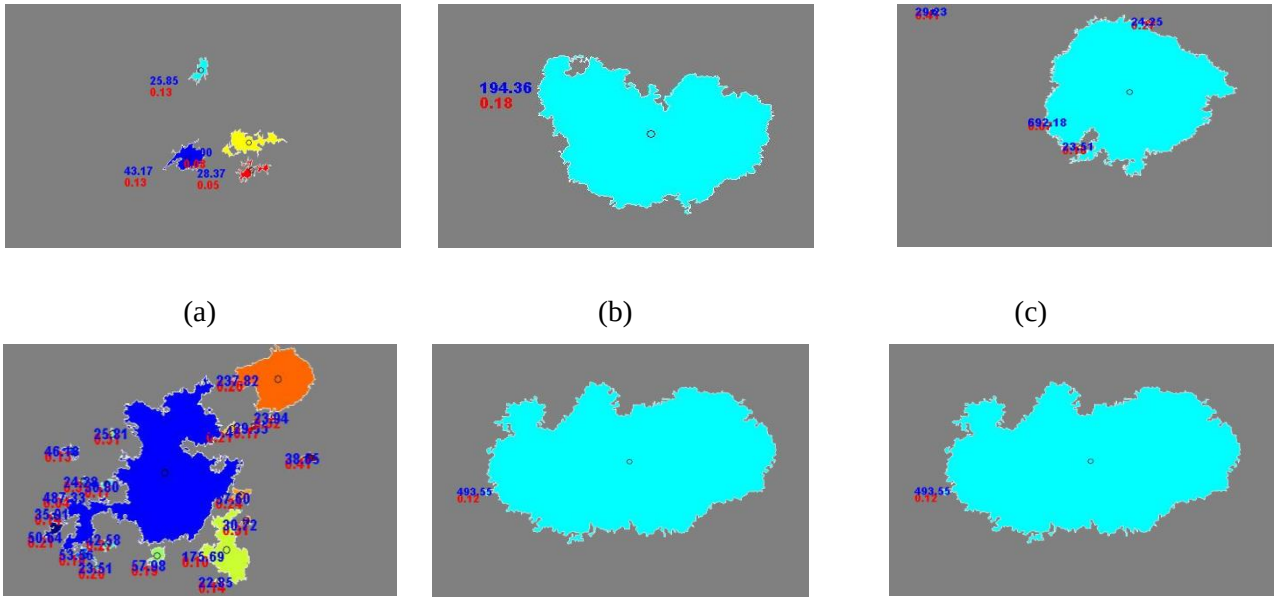

(a) (b) (c)

(d) (e) (f)

Figure 8 Example of metric calculated images

Metric is calculated on the basis of roundness and diameter. In figure 8 metric is calculated for all images. Metric value greater than 60 indicates that melanoma is detected.

The Haralick's texture features are statistics calculated on grey level co-occurrence matrix derived from each image. Table 1 shows the obtained results for Haralick features on dataset.

Table 1 Classification Performance of Haralick's on Dataset

NUMBER OF FEATURES	ACCURACY RATE
286	71%

SIFT (Scale Invariant Feature Transform) extracts texture features from an image. Table 2 shows the obtained results for SIFT and DSIFT (Dense SIFT) on dataset.

Table 2 Classification Performance of SIFT on Dataset

Vocabulary Size	Number of Features	Accuracy of DSIFT	Accuracy of SIFT
100	100	52.5%	50.3%
300	300	59.3%	56.1%
500	500	61.5%	58.0%
700	700	63.0%	59.2%
900	900	62.5%	59.3%
Combined Vocabulary (100+300+500+900)	1800	66.7%	63.1%

Experiments for LTP carried using the same number of neighbors and same size of radius as in the case of the local binary pattern (LBP). Table 4.3 describes the classification results for LTP.

Table 3 Classification Performance of LTP

Radius	Neighbors	Number of Features	Accuracy Rate
1	8	118	38.0%
2	16	486	47.3%
2	24	1110	51.3%
3	24	1110	53.4%
Combined	Combined	2824	55.0%

Combined color histogram for all the three-color channels obtained 29.2%. Table 3 describes the obtained results for the color histogram.

Table 3 Classification Performance of Color Histogram

Number of Features	Accuracy Rate
768	29.2%

Table 4 shows the average performance of the proposed model in term of accuracy, precision, recall and F-score

Overall Accuracy	Average Precision	Average Recall	Average F Score
85.5	0.87	0.89	86.90

The performance of proposed framework is compared with other frameworks mentioned in the literature. Comparison with existing approaches shows that our proposed method provides better results. Leo et al. [8] in 2008

get specificity and sensitivity of 85% in their proposed work. Alcon et al. [10] get accuracy of 84% with a sensitivity of 94%, and specificity of 68%. Barata et al. [12] get specificity and sensitivity of the system is 82.1% and 91.1%. Christensen et al. [14] get accuracy of 77%. Lyatomi et al. [19], their system achieves sensitivity of 85.9% and specificity of 86%. Proposed System provides the precision of .87 and recall of .89. Our proposed system provides accuracy of 85.5%.

4. Conclusion

In this work, an improved procedure for detection of melanoma is proposed based on pigment network in dermoscopic images. Initially image is converted into gray scale image and then into binary image. Binary mask is created for binary image and then it is changed into final binary mask to detect melanoma by calculating its diameter and radius. At the end pigmented network present in the skin lesion images is detected. Feature extracted are also described with their accuracy. Haralick features have accuracy of 71%. SIFT and DSIFT features have accuracy of 63 and 66.7% respectively. Local ternary pattern features have accuracy of 55% and color histogram features have accuracy of 29.2%. Average precision was .89 and average recall was .87. The experiments are carried out on various dermoscopic images in order to check algorithm's efficiency. Proposed method shows the overall accuracy of 85.5%. In future, more features will be extracted in order to improve the algorithm's detection and accuracy for melanoma diagnosis.

Reference

[1] "World Health Organization", World Health Organization, 2017. [Online]. Available: http://www.who.int. [Accessed: 08- Jan- 2017].

[2] Raza, A., & Meeran, M. T. (2019). Routine of encryption in cognitive radio network. Mehran University Research Journal of Engineering & Technology, 38(3), 609-618.

[3] Khan, S.U.R.; Zhao, M.; Asif, S.; Chen, X.; Zhu, Y. GLNET: Global–local CNN's-based informed model for detection of breast cancer categories from histopathological slides. J. Supercomput. 2023, 80, 7316–7348.

[4] D.J. Gawkrodger. Dermatology: an illustrated colour text. Elsevier Health Sciences, 2002

[5] Khan, S.U.R.; Zhao, M.; Asif, S.; Chen, X. Hybrid-NET: A fusion of DenseNet169 and advanced machine learning classifiers for enhanced brain tumor diagnosis. Int. J. Imaging Syst. Technol. 2024, 34, e22975.

[6] Khan, S.U.R.; Asif, S.; Bilal, O.; Ali, S. Deep hybrid model for Mpox disease diagnosis from skin lesion images. Int. J. Imaging Syst. Technol. 2024, 34, e23044.

[7] Khan, S. U. R., & Asif, S. (2024). Oral cancer detection using feature-level fusion and novel self-attention mechanisms. Biomedical Signal Processing and Control, 95, 106437.

[8] Waqas, M., Khan, Z., Ahmed, S. U., & Raza, A. (2023, November). MIL-Mixer: a robust bag encoding strategy for Multiple Instance Learning (mil) using MLP-Mixer. In 2023 18th International Conference on Emerging Technologies (ICET) (pp. 22-26). IEEE.

[9] Raza, A., Soomro, M. H., Shahzad, I., & Batool, S. (2024). Abstractive Text Summarization for Urdu Language. Journal of Computing & Biomedical Informatics, 7(02).

[10] J. Fernandez Alcon, C. Ciuhu, W. ten Kate, A. Heinrich, N. Uzunbajakava, G. Krekels, D. Siem and G. de Haan, "Automatic Imaging System With Decision Support for Inspection of Pigmented Skin Lesions and Melanoma Diagnosis", IEEE Journal of Selected Topics in Signal Processing, vol. 3, no. 1, pp. 14-25, 2009.

[11] Farooq, M. U., & Beg, M. O. (2019, November). Bigdata analysis of stack overflow for energy consumption of android framework. In 2019 International Conference on Innovative Computing (ICIC) (pp. 1-9). IEEE.

[12] Dai, Q., Ishfaque, M., Khan, S. U. R., Luo, Y. L., Lei, Y., Zhang, B., & Zhou, W. (2024). Image classification for sub-surface crack identification in concrete dam based on borehole CCTV images using deep dense hybrid model. Stochastic Environmental Research and Risk Assessment, 1-18.

[13] M. Celebi, H. Kingravi, B. Uddin, H. Iyatomi, Y. Aslandogan, W. Stoecker and R. Moss, "A methodological approach to the classification of dermoscopy images", Computerized Medical Imaging and Graphics, vol. 31, no. 6, pp. 362-373, 2007.

[14] J. Christensen, M. Soerensen, Z. Linghui, S. Chen and M. Jensen, "Pre-diagnostic digital imaging prediction model to discriminate between malignant melanoma and benign pigmented skin lesion", Skin Research and Technology, vol. 16, no. 1, pp. 98-108, 2010.

[15] Shahzad, I., Khan, S. U. R., Waseem, A., Abideen, Z. U., & Liu, J. (2024). Enhancing ASD classification through hybrid attention-based learning of facial features. Signal, Image and Video Processing, 1-14.

[16] Khan, U. S., & Khan, S. U. R. (2024). Boost diagnostic performance in retinal disease classification utilizing deep ensemble classifiers based on OCT. Multimedia Tools and Applications, 1-21.

[17] Khan, M. A., Khan, S. U. R., Haider, S. Z. Q., Khan, S. A., & Bilal, O. (2024). Evolving knowledge representation learning with the dynamic asymmetric embedding model. Evolving Systems, 1-16.

[18] Khan, U. S., Ishfaque, M., Khan, S. U. R., Xu, F., Chen, L., & Lei, Y. (2024). Comparative analysis of twelve transfer learning models for the prediction and crack detection in concrete dams, based on borehole images. Frontiers of Structural and Civil Engineering, 1-17.

[19] H. Iyatomi, H. Oka, M. Celebi, M. Hashimoto, M. Hagiwara, M. Tanaka and K. Ogawa, "An improved Internet-based melanoma screening system with dermatologist-like tumor area extraction algorithm", Computerized Medical Imaging and Graphics, vol. 32, no. 7, pp. 566-579, 2008.

[20] H. Iyatomi, H. Oka, M. Saito, A. Miyake, M. Kimoto, J. Yamagami, S. Kobayashi, A. Tanikawa, M. Hagiwara, K. Ogawa, G. Argenziano, H. Peter Soyer and M. Tanaka, "Quantitative assessment of tumour extraction from dermoscopy images and evaluation of computer-based extraction methods for an automatic melanoma diagnostic system", Melanoma Research, vol. 16, no. 2, pp. 183-190, 2006.

[21] Al-Khasawneh, M. A., Raza, A., Khan, S. U. R., & Khan, Z. (2024). Stock Market Trend Prediction Using Deep Learning Approach. Computational Economics, 1-32.

[22] Rein-Lien Hsu, M. Abdel-Mottaleb and A. Jain, "Face detection in color images", IEEE Transactions on Pattern Analysis and Machine Intelligence, vol. 24, no. 5, pp. 696-706, 2002.

[23] Raza, A.; Meeran, M.T.; Bilhaj, U. Enhancing Breast Cancer Detection through Thermal Imaging and Customized 2D CNN Classifiers. VFAST Trans. Softw. Eng. 2023, 11, 80–92.

[24] Khan, S.U.R.; Zhao, M.; Asif, S.; Chen, X.; Zhu, Y. GLNET: Global–local CNN's-based informed model for detection of breast cancer categories from histopathological slides. J. Supercomput. 2023, 80, 7316–7348.

[25] Khan, S.U.R.; Asif, S.; Bilal, O.; Ali, S. Deep hybrid model for Mpox disease diagnosis from skin lesion images. Int. J. Imaging Syst. Technol. 2024, 34, e23044.

[26] Khan, S.U.R.; Zhao, M.; Asif, S.; Chen, X. Hybrid-NET: A fusion of DenseNet169 and advanced machine learning classifiers for enhanced brain tumor diagnosis. Int. J. Imaging Syst. Technol. 2024, 34, e22975.

[27] Farooq, M.U.; Beg, M.O. Bigdata analysis of stack overflow for energy consumption of android framework. In Proceedings of the 2019 International Conference on Innovative Computing (ICIC), Lahore, Pakistan, 1–2 November 2019; pp. 1–9.

[28] S. Fischer, P. Schmid and J. Guillod, "Analysis of skin lesions with pigmented networks" Image Processing, Proceeding of International Conference on. Vol. 1. IEEE, 1996.

[29] Khan, S.U.R.; Raza, A.;Waqas, M.; Zia, M.A.R. Efficient and Accurate Image Classification Via Spatial Pyramid Matching and SURF Sparse Coding. Lahore Garrison Univ. Res. J. Comput. Sci. Inf. Technol. 2023, 7, 10–23.